

## Many-Body Theory of Ultrafast Demagnetization and Angular Momentum Transfer in Ferromagnetic Transition Metals

W. Töws and G. M. Pastor

*Institut für Theoretische Physik, Universität Kassel, Heinrich-Plett-Straße 40, 34132 Kassel, Germany*  
(Received 12 June 2015; published 20 November 2015)

Exact calculated time evolutions in the framework of a many-electron model of itinerant magnetism provide new insights into the laser-induced ultrafast demagnetization observed in ferromagnetic (FM) transition metal thin films. The interplay between local spin-orbit interactions and interatomic hopping is shown to be at the origin of the observed postexcitation breakdown of FM correlations between highly stable local magnetic moments. The mechanism behind spin- and angular-momentum transfer is revealed from a microscopic perspective by rigorously complying with all fundamental conservation laws. An energy-resolved analysis of the time evolution shows that the efficiency of the demagnetization process reaches almost 100% in the excited states.

DOI: [10.1103/PhysRevLett.115.217204](https://doi.org/10.1103/PhysRevLett.115.217204)

PACS numbers: 75.78.Jp, 75.10.Lp, 75.70.Ak, 75.70.Tj

Pump-and-probe femtosecond-laser experiments on thin magnetic transition metal (TM) films have shown, almost 2 decades ago, that ferromagnetic (FM) order breaks down on a time scale of a few hundred femtoseconds after the pulse absorption [1]. This remarkable finding opened the way to an ever growing research field, which has wide fundamental and practical importance [2–12]. The phenomenon as such can be neither an immediate consequence of the excitation, since optical transitions conserve spin, nor the result of thermally activated stochastic processes, which would involve a much longer time scale. Instead, ultrafast demagnetization (UFD) reflects the intrinsic many-body dynamics of correlated excited electrons in FM metals. Understanding its origin and controlling its properties is therefore of crucial importance [13].

From a fundamental perspective, it has been clear from the start that spin-orbit (SO) interactions must play a central role in the dynamics, since only the relativistic corrections break the conservation of the total electronic spin [4,14,15]. Indeed, the spin-orbit coupling (SOC) allows exchanges between the dominant local  $3d$  spin moments  $\vec{s}_i$  and the local orbital moments  $\vec{l}_i$  at every TM atom  $i$ . Taking into account that the total angular momentum  $\vec{j}_i = \vec{l}_i + \vec{s}_i$  is conserved in this process, the focus of attention quickly moved towards quantifying the time dependences of the spin and orbital moments, and correlating them to the observed demagnetization. This has been experimentally achieved by performing time-resolved x-ray magnetic circular dichroism (XMCD) measurements on Ni [7,10,16]. These works showed, in contrast to early expectations, that no enhancement of  $l_{iz}$  accompanies the decrease of  $s_{iz}$ , but rather that both  $s_{iz}$  and  $l_{iz}$  decrease as a function of time with a time constant of  $\tau \approx 120$  fs. Since  $\vec{l}_i$  is not a reservoir for angular momentum, the authors concluded that a femtosecond spin-lattice relaxation, i.e., a substantial femtosecond spin angular momentum transfer to the lattice, takes place [7].

Although the theoretical research in this field has been most intense, understanding the microscopic mechanisms of UFD and angular-momentum relaxation still remains an open problem [17]. Over the past years, two different theoretical approaches have attracted particular attention. One of them is electron-phonon spin-flip scattering, in which the lattice is assumed to be a perfect sink for angular momentum [18–22]. The other one is spin-polarized electron diffusion, which does not invoke any angular momentum dissipation channel, but rather a spin-dependent superdiffusive electron transport from the laser-excited film to the substrate [23–26]. In this context, it is quite remarkable that none of these theories happens to bear a clear relation to the fundamentals of itinerant magnetism, which are tightly anchored to strong electron correlations and to the resulting high stability of the local  $3d$  magnetic moments [27]. Only recently has the potential importance of localized spins and their fluctuations been suggested [29,30]. It is therefore most challenging to establish the links between equilibrium and nonequilibrium theories of itinerant magnetism. The purpose of this Letter is to develop a many-body theory of UFD, which takes into account the electronic correlations responsible for local moment formation and magnetic order, and to analyze its physical consequences rigorously by performing exact time propagations.

Several distinct features are expected to be central to the physics of the laser-excited electrons in FM metals: (i) the single-particle hybridizations responsible for electron delocalization, bonding and metallic behavior, (ii) the dominant Coulomb interactions among the  $3d$  electrons, which introduce correlations, stabilize the local magnetic moments and, together with the single-particle contributions, define the magnetic order, (iii) the SO interactions, which couple the spin and orbital degrees of freedom, and (iv) the interaction with the external laser field, which

triggers the initial electronic excitation. We therefore propose the  $pd$ -band model given by

$$\hat{H} = \hat{H}_0 + \hat{H}_C + \hat{H}_{SO} + \hat{H}_E(t), \quad (1)$$

where

$$\hat{H}_0 = \sum_{i\alpha\sigma} \epsilon_\alpha \hat{n}_{i\alpha\sigma} + \sum_{ij} \sum_{\alpha\beta\sigma} t_{ij}^{\alpha\beta} \hat{c}_{i\alpha\sigma}^\dagger \hat{c}_{j\beta\sigma} \quad (2)$$

describes the band structure of the relevant  $3d$  and  $4p$  valence electrons that are responsible for the magnetic properties in TMs and for the relevant optical absorption. The operator  $\hat{c}_{i\alpha\sigma}^\dagger$  ( $\hat{c}_{i\alpha\sigma}$ ) creates (annihilates) a spin- $\sigma$  electron at atom  $i$  in the orbital  $\alpha$ , which has well-defined radial and orbital quantum numbers  $n\ell m$ .  $\hat{n}_{i\alpha\sigma} = \hat{c}_{i\alpha\sigma}^\dagger \hat{c}_{i\alpha\sigma}$  counts the corresponding occupations. The energy of the orbital  $\alpha$  is denoted by  $\epsilon_\alpha$  and the interatomic hopping integrals by  $t_{ij}^{\alpha\beta}$ . The second term in Eq. (1) designates the dominant intra-atomic Coulomb interaction among the  $3d$  electrons:

$$\hat{H}_C = \frac{U}{2} \sum_i \hat{n}_i^d (\hat{n}_i^d - 1) - J \sum_i \hat{s}_i^d \cdot \hat{s}_i^d, \quad (3)$$

where  $U$  stands for the average  $d$ -electron direct Coulomb integral and  $J$  for the exchange integral [31,32]. The operators  $\hat{n}_i^d$  and  $\hat{s}_i^d$  refer, respectively, to the  $d$ -electron number and total spin at atom  $i$ . The spin-orbit interactions are given by the third term

$$\hat{H}_{SO} = \xi \sum_i \sum_{\alpha\beta\in 3d} \sum_{\sigma\sigma'} (\vec{l} \cdot \vec{s})_{\alpha\sigma, \beta\sigma'} \hat{c}_{i\alpha\sigma}^\dagger \hat{c}_{i\beta\sigma'}, \quad (4)$$

where  $(\vec{l} \cdot \vec{s})_{\alpha\sigma, \beta\sigma'}$  stands for the intra-atomic matrix elements of  $\vec{l} \cdot \vec{s}$  and  $\xi$  is the SOC constant. For simplicity,  $4p$  electrons are here ignored. Finally, the last term

$$\hat{H}_E(t) = e\vec{E}(t) \cdot \sum_{i\alpha\beta\sigma} \langle \alpha | \hat{r} | \beta \rangle \hat{c}_{i\alpha\sigma}^\dagger \hat{c}_{i\beta\sigma} \quad (5)$$

describes the interaction with the external laser field  $\vec{E}(t)$  in the intra-atomic dipole approximation ( $e > 0$  is the electron charge). The usual atomic selection rules for the position operator  $\hat{r}$  imply that only  $dp$  and  $pd$  transitions enter the sum.

At this point it is useful to recall the fundamental conservation laws underlying the model, which are the same as in the first-principles Hamiltonian. The nonrelativistic terms  $\hat{H}_0$ ,  $\hat{H}_C$ , and  $\hat{H}_E$  conserve the total spin  $\vec{S} = \sum_{i\alpha} \vec{s}_{i\alpha}$ , since  $[\hat{H}_0, \vec{S}] = [\hat{H}_C, \vec{S}] = [\hat{H}_E, \vec{S}] = 0$ . The spin conservation is broken only by  $\hat{H}_{SO} \propto \sum_i [(l_{i+} s_{i-} + l_{i-} s_{i+})/2 + l_{iz} s_{iz}]$ , which involves intra-atomic angular-momentum transfer between  $\vec{s}_i$  and  $\vec{l}_i$ .

Still, the total angular momentum  $\vec{j}_i = \vec{l}_i + \vec{s}_i$  is locally conserved in the SO transitions, since  $[\hat{H}_{SO}, \vec{s}_i + \vec{l}_i] = 0$  for any atom  $i$ . Intra-atomic Coulomb interactions are also invariant upon rotations and thus preserve  $\vec{s}_i$ ,  $\vec{l}_i$ , and  $\vec{j}_i$ . However, the interatomic hybridizations, though total-spin conserving, do not preserve the orbital angular momentum  $\vec{L} = \sum_{i\alpha} \vec{l}_{i\alpha}$ , since the hopping integrals  $t_{ij}^{\alpha\beta}$  connect orbitals having different  $m$  at different atoms ( $[\hat{H}_0, \vec{L}] \neq 0$  and  $[\hat{H}_0, \vec{l}_i] \neq 0$ ) [33]. We shall see that these simple arguments allow us to understand a number of qualitative aspects of the magnetization dynamics, its dependence on the relevant physical parameters, and the main mechanism behind it.

Despite the simplicity and transparency of the proposed  $pd$ -band model, an analytical or straightforward numerical solution of its dynamics is out of reach at present. As in the equilibrium case, the main difficulties stem from the Coulomb interaction  $\hat{H}_C$  and the resulting many-body behavior. One could, in principle, resort to time-dependent mean-field approximations. However, these are known to introduce artificial symmetry breakings, which spoil the fundamental spin rotational invariance, thus casting potentially serious doubts on the resulting magnetization dynamics. In order to derive rigorous conclusions, we have therefore decided to consider a simplified small-cluster version of the model and to obtain an exact numerical solution of the ground state, excitations, and time propagation. Similar approaches have been most successful in the context of equilibrium properties of narrow-band systems [34–36]. In addition, our results show that the physics of the magnetization dynamics can be explained by short-range effects, which justifies the small-cluster approach *a posteriori*.

The parameters used for the calculations correspond approximately to Ni and have been specified as follows. The nearest-neighbor (NN) Slater-Koster hopping integrals are taken from band structure calculations [37]. The  $dp$  promotion energy  $\Delta\epsilon_{pd} = 1$  eV yields a dominant  $3d$  band occupation in the ground state. The direct Coulomb integral  $U = 4.5$  eV and the exchange integral  $J = 0.8$  eV lead to FM order with nearly saturated  $3d$  moments at low temperatures [34]. Finally, the SOC constant  $\xi$  is varied in the range  $|\xi| \leq 100$  meV, which includes the values found in  $3d$  TMs [38]. For the numerical calculations we reduce the degeneracy of the bands, by considering only three  $3d$  orbitals per atom (having  $m = -1, 0$ , and  $1$ ) and one  $4p$  orbital per atom ( $m = 0$ ). The fcc (111) monolayer is modeled by an equilateral triangle having  $N_e = 4$  valence electrons. Since the average occupation of the  $d$  orbitals is below half-band filling ( $\langle \hat{n}_{i\alpha}^d \rangle \approx N_e/3N_a = 0.44$ ), we set  $\xi < 0$  in order that  $\vec{s}_i$  and  $\vec{l}_i$  align parallel to each other [40].

A first test on the validity of the model and parameter choice is provided by the ground-state results, which match

qualitatively the magnetic properties of Ni. From exact Lanczos diagonalizations we obtain that the ground state is FM with an off-plane easy magnetization axis and a magnetic anisotropy energy  $\Delta E = 2.8$  meV per atom. The local spin momenta  $2s_{iz} = 1.32\hbar$  are almost saturated, whereas the local orbital momenta  $l_{iz} = 0.09\hbar$  are quenched to a large extent. These values should be compared, for example, with  $2s_{iz} = 0.62\hbar$  and  $l_{iz} = 0.07\hbar$  obtained in experiment [10].

Starting from the FM ground state we determine the exact time evolution numerically by performing short-time iterative Lanczos propagations [41]. The actual dynamics is triggered by the femtosecond laser pulse  $\vec{E}(t) = \vec{e} E_0 \cos(\omega t) \exp(-t^2/\tau_p^2)$ , whose polarization vector  $\vec{e}$  is along a NN bond within the (111) plane. The laser wavelength  $\lambda = 800$  nm corresponds to the photon energy  $\hbar\omega = 1.55$  eV used in several experiments [2,4,6,7,9,10]. The pulse is centered at  $t = 0$  and has a duration of  $\tau_p = 5$  fs. Its amplitude  $E_0$  is such that the electronic system absorbs 0.2 photons per atom on average, which corresponds to a fluence  $F \approx 40$  mJ/cm<sup>2</sup> [42].

In Fig. 1 results are given for the magnetization dynamics. For realistic values of  $|\xi| = 50$ –100 meV the spin angular momentum per atom relaxes irreversibly from  $2S_z/N_a = 1.32\hbar$  to around  $0.64\hbar$  within the first hundreds of femtoseconds following the laser excitation. This demonstrates the ultrafast demagnetization effect in agreement with experiment [7]. Figure 1 also reveals the central role played by the SOC. For  $\xi = 0$  the total spin is unaffected by the optical excitation, as expected. Moreover, as the SOC is turned on one observes that the degree of demagnetization  $\Delta S_z = S_z(0) - S_z(\infty)$  increases and that the demagnetization time  $\tau_{dm}$  decreases. Finally, for larger  $|\xi| \geq 50$  meV the SOC strength affects only the time scale. In order to quantify  $\tau_{dm}$ , we have fitted the exact time dependence

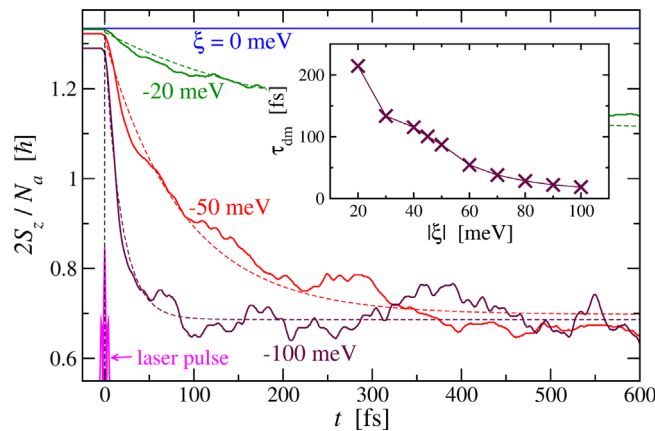


FIG. 1 (color online). Time dependence of the spin magnetization  $2S_z$  following a 5 fs laser-pulse excitation for an equilateral triangle having  $N_e = 4$  valence electrons and different SOC strengths  $\xi$ . The inset shows the demagnetization time  $\tau_{dm}$  as a function of  $\xi$ .

$S_z(t)$  with an exponential function of the form  $\tilde{S}_z(t) = \Delta S_z \exp(-t/\tau_{dm}) + S_z(0) - \Delta S_z$ , which is shown by the dashed curves in Fig. 1. The obtained  $\tau_{dm}$ , shown in the inset, behaves approximately as  $\tau_{dm} \approx 6\hbar/|\xi|$ . This is consistent with the time-energy uncertainty relation and confirms that the SOC, which represents the smallest energy scale, controls the time scale of the relaxation process.

The time dependences of the local  $d$ -electron spin moments  $\mu_i^d = \sqrt{\langle (\vec{s}_i^d)^2 \rangle}$  and of the NN spin correlation functions  $\gamma_{ij} = \langle \vec{s}_i^d \cdot \vec{s}_j^d \rangle$  shown in Fig. 2 for  $\xi = -50$  meV provide a much clearer picture of how the UFD actually occurs. One observes that  $\mu_i$  changes very slightly from  $1.04\hbar$  to  $0.98\hbar$  while the laser pulse is on ( $\tau_p = 5$  fs). This is the result of a small laser-induced  $dp$  charge transfer, which involves majority  $d$  electrons, and which causes the number of  $d$  electrons per atom to decrease from  $n_d \approx 1.25$  to  $n_d \approx 1.17$ . Otherwise,  $\mu_i^d$  is essentially time independent. The remarkable stability of the local  $d$  moments shows, as in thermal equilibrium above the Curie temperature  $T_C$ , that the laser-induced ultrafast breakdown of FM order is not the consequence of a significant loss of local spin polarization [27]. Instead, the UFD follows to a large extent from the quantum fluctuations of the orientations of the local magnetic moments  $\vec{s}_i^d$ , whose magnitude remains almost constant throughout the process. Indeed, as shown in Fig. 2, the average NN spin-correlation function  $\gamma_{ij}$  decreases very rapidly as a function of time, approaching its long-time limit already 50–80 fs after the laser absorption, and remaining approximately constant in the following. The breakdown of the NN correlations is actually much more rapid than the decrease of the total spin polarization  $S_z$  (see Fig. 2). The same trend holds for other values of  $\xi$ , for example  $\xi = -100$  meV, where the demagnetization time is much shorter. This shows that the quantum fluctuations of  $\vec{s}_i^d$  dominate only the first stages of the spin dynamics. A

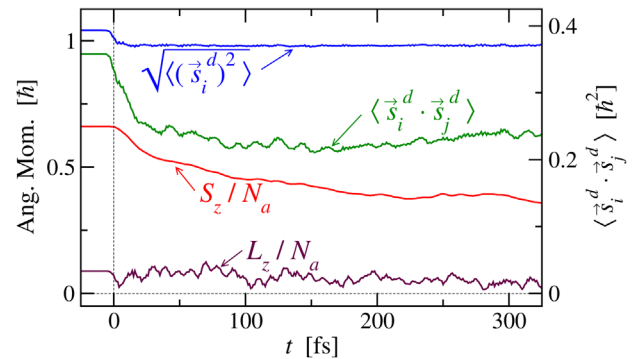


FIG. 2 (color online). Time dependence of the average  $d$ -electron local spin moment  $\langle (\vec{s}_i^d)^2 \rangle^{1/2}$ , NN spin-spin correlation function  $\langle \vec{s}_i^d \cdot \vec{s}_j^d \rangle$ , and off-plane spin and orbital angular momentum  $S_z$  and  $L_z$ .



slower tilting of  $\vec{S}$  off the  $z$  axis follows, during which the transversal components  $S_x$  and  $S_y$  always remain zero.

In order to analyze the mechanisms of angular-momentum transfer behind the UFD process, we turn our attention to the dynamics of the orbital moment  $L_z$  and contrast it with the dynamics of  $S_z$  (see Fig. 2). In the ground state, before the laser excitation,  $L_z/N_a \approx 0.09\hbar$  is quenched to a large extent in comparison with the Hund-rule atomic value  $L_z^{\text{at}} = 1\hbar$ , as expected in TMs. After the excitation,  $L_z/N_a$  shows rapid oscillations between  $0.02\hbar$  and  $0.12\hbar$ , always remaining parallel to  $S_z$ . This oscillatory behavior is numerically stable and perfectly reproducible. The total angular momentum  $J_z = L_z + S_z$  is obviously not a constant of motion. This is in agreement with time-resolved XMCD experiments showing that  $L_z$  is not a reservoir for the decreasing  $S_z$  [7,10,16]. The fact that  $L_z$  remains quenched for all times is the result of the interatomic hybridizations responsible for the electronic motion in the lattice and for the band formation. Formally, one could say that the operator  $\hat{H}_0$  preserves  $\vec{S}$  but not  $\vec{L}$  (i.e.,  $[\hat{H}_0, \vec{S}] = 0$  while  $[\hat{H}_0, \vec{L}] \neq 0$ ) since the potential generated by the ions is not rotationally invariant [43]. But physically it is important to realize that the characteristic time  $\tau_q$  required to quench the orbital moment of an electron in a lattice is extremely short, of the order of  $\tau_q \sim \hbar/W_d \approx 0.1$  fs, where  $W_d \approx 6$  eV stands for the  $d$ -band width [44]. The combination of a local  $\vec{J}$ -conserving transfer of angular momentum from  $\vec{S}$  to  $\vec{L}$ , due to SO interactions, and a very fast dynamical quenching of  $\vec{L}$ , due to electronic hopping, explains the spin-to-lattice angular-momentum transfer observed in experiment. In the framework of the present model, the dynamical quenching of  $L$  would manifest itself only as a global rotation of the rigid lattice, since electron-phonon coupling (EPC) has been neglected. Including EPC in the model would open an additional channel for  $L$  quenching, through which angular momentum would be transferred to the lattice vibrations.

In order to verify the validity of our conclusions we have repeated the calculations of the dynamics by reducing artificially the hopping integrals  $t_{ij}^{\alpha\beta}$  and thus approaching the atomic zero-band-width limit. As shown in the Supplemental Material, one observes that as soon as  $t_{ij}^{\alpha\beta}$  becomes comparable or smaller than the SOC constant  $\xi$  the rapid quenching of  $L_z$  is replaced by oscillations of both  $L_z$  and  $S_z$ , with a period of about 70 fs, during which  $J_z$  is approximately conserved [45].

A complementary perspective to the UFD process is obtained by performing a spectral analysis of the laser-excited many-body state  $\Psi(t)$  and of the time dependence of  $S_z$ . For this purpose, we considered  $\Psi(t)$  immediately after the excitation (at  $t = 3\tau_p$ ) and expanded it in the stationary states  $\psi_k$  of the field-free Hamiltonian  $\hat{H} = \hat{H}_0 + \hat{H}_C + \hat{H}_{\text{SO}}$  having energy  $\varepsilon_k$ . The obtained spectral

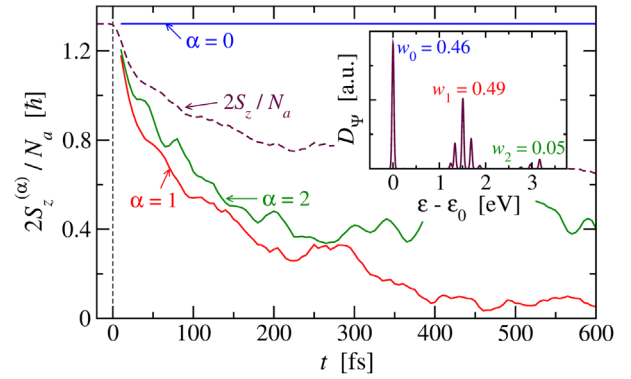


FIG. 3 (color online). Time dependence of the spin magnetization  $2S_z^{(\alpha)}$  in the excited-state manifolds corresponding to  $\alpha = 0, 1$ , and  $2$  photon absorptions ( $\hbar\omega = 1.55$  eV). The average  $S_z = \sum_{\alpha} w_{\alpha} S_z^{(\alpha)}$  is given by the dashed curve. The inset shows the spectral distribution  $D_{\Psi}(\varepsilon)$  of  $\Psi(t)$  after the laser-pulse passage ( $t \geq 3\tau_p = 15$  fs). The weights  $w_{\alpha}$  of the different spectral parts of  $\Psi$  are indicated.

distribution  $D_{\Psi}(\varepsilon) = \sum_k \delta(\varepsilon - \varepsilon_k) |\langle \psi_k | \Psi \rangle|^2$  is shown in the inset of Fig. 3. Notice that  $D_{\Psi}(\varepsilon)$  is independent of  $t$  after the pulse passage, as is  $\hat{H}$  [see Eqs. (1)–(5)]. Three main groups or manifolds of nearby peaks can be recognized, which are located at the excitation energies  $\Delta\varepsilon \approx \alpha\hbar\omega$  and which correspond to the absorption of  $\alpha = 0, 1$ , and  $2$  photons. The spin magnetization  $S_z^{(\alpha)}$  originating from these manifolds is shown in Fig. 3 as a function of  $t$ . One observes that immediately after excitation all  $\alpha$  have the same saturated magnetization. This simply reflects the spin conservation upon optical dipole transitions. The ground state, being a pure stationary state, preserves  $\langle \hat{S}_z \rangle$  and yields a time-independent  $S_z^{(0)}$ . Relaxation can only stem from the excitations. Indeed, in the excited manifolds  $S_z^{(\alpha)}$  decreases dramatically to nearly zero, particularly in the most relevant  $\alpha = 1$  manifold. This demonstrates the remarkably high efficiency of laser-induced UFD in the excited states. The residual average magnetization  $2S_z(t \rightarrow \infty)$ , which persists after the relaxation process (see Fig. 1), is essentially the consequence of the finite overlap between the many-body state  $\Psi(t)$  after the laser absorption and the ground state.

In sum, the laser-induced magnetization dynamics of ferromagnetic TMs has been studied in the framework of an electronic model. For the first time a solution of the time-dependent many-body problem has been achieved, which is complete from the perspectives of electron correlations, spin-orbit interactions, and essential symmetries. The results have demonstrated that the femtosecond demagnetization can be explained in terms of a three-step mechanism: (i) The laser pulse creates electron-hole pairs. This opens the way for (ii) the SOC, yielding local angular-momentum transfer from  $\vec{s}_i$  to  $\vec{l}_i$  with a characteristic time scale of  $\hbar/|\xi| \approx 10$  fs. However, angular momentum is not

accumulated in  $\vec{l}_i$ , since (iii)  $\vec{L}$  is quenched by the motion of electrons in the lattice. This takes place on a much shorter time scale of only  $\hbar/W_d \lesssim 1$  fs. Extensions of this work by improving the model Hamiltonian are certainly desirable and necessary for a more realistic description of specific magnetic materials. In particular, the coexistence of different relaxation channels (electronic relaxation, electron-phonon spin-flip scattering, spin diffusion, etc.) deserves to be explored. In any case, the simplicity of the electronic processes identified in this work and the fundamental character of the proposed model suggest that the rigorously derived concepts should be universally applicable.

W. T. acknowledges the support provided by the Otto-Braun Foundation. Computer resources were supplied by the IT Service Center of the University of Kassel and by the Center for Scientific Computing of the University of Frankfurt.

- 
- [1] E. Beaupaire, J.-C. Merle, A. Daunois, and J.-Y. Bigot, *Phys. Rev. Lett.* **76**, 4250 (1996).
- [2] J. Hohlfeld, E. Matthias, R. Knorren, and K. H. Bennemann, *Phys. Rev. Lett.* **78**, 4861 (1997).
- [3] B. Koopmans, M. van Kampen, J. T. Kohlhepp, and W. J. M. de Jonge, *Phys. Rev. Lett.* **85**, 844 (2000).
- [4] H.-S. Rhie, H. A. Dürr, and W. Eberhardt, *Phys. Rev. Lett.* **90**, 247201 (2003).
- [5] M. Lisowski, P. A. Loukakos, A. Melnikov, I. Radu, L. Ungureanu, M. Wolf, and U. Bovensiepen, *Phys. Rev. Lett.* **95**, 137402 (2005).
- [6] M. Cinchetti, M. Sánchez Albaneda, D. Hoffmann, T. Roth, J.-P. Wüstenberg, M. Krauß, O. Andreyev, H. C. Schneider, M. Bauer, and M. Aeschlimann, *Phys. Rev. Lett.* **97**, 177201 (2006).
- [7] C. Stamm, T. Kachel, N. Pontius, R. Mitzner, T. Quast, K. Holldack, S. Khan, C. Lupulescu, E. F. Aziz, M. Wietstruk, H. A. Dürr, and W. Eberhardt, *Nat. Mater.* **6**, 740 (2007).
- [8] C. D. Stanciu, F. Hansteen, A. V. Kimel, A. Kirilyuk, A. Tsukamoto, A. Itoh, and Th. Rasing, *Phys. Rev. Lett.* **99**, 047601 (2007).
- [9] E. Carpene, E. Mancini, C. Dallera, M. Brenna, E. Puppini, and S. De Silvestri, *Phys. Rev. B* **78**, 174422 (2008).
- [10] C. Stamm, N. Pontius, T. Kachel, M. Wietstruk, and H. A. Dürr, *Phys. Rev. B* **81**, 104425 (2010).
- [11] I. Radu, K. Vahaplar, C. Stamm, T. Kachel, N. Pontius, H. A. Dürr, T. A. Ostler, J. Barker, R. F. L. Evans, R. W. Chantrell, A. Tsukamoto, A. Itoh, A. Kirilyuk, Th. Rasing, and A. V. Kimel, *Nature (London)* **472**, 205 (2011).
- [12] N. Bergerd, V. Lopez-Flores, V. Halte, M. Hehn, C. Stamm, N. Pontius, E. Beaupaire, and C. Boeglin, *Nat. Commun.* **5**, 3466 (2014).
- [13] A. Kirilyuk, A. V. Kimel, and T. Rasing, *Rev. Mod. Phys.* **82**, 2731 (2010).
- [14] G. P. Zhang and W. Hübner, *Phys. Rev. Lett.* **85**, 3025 (2000).
- [15] J.-Y. Bigot, E. Beaupaire, L. Guidoni, and J.-C. Merle, in *Magnetism: Molecules to Materials III*, edited by J. S. Miller and M. Drillon (Wiley-VCH Verlag, Weinheim, 2002).
- [16] C. Boeglin, E. Beaupaire, V. Halté, V. López-Flores, C. Stamm, N. Pontius, H. A. Dürr, and J.-Y. Bigot, *Nature (London)* **465**, 458 (2010).
- [17] E. Turgut, C. La-o-vorakiat, J. M. Shaw, P. Grychtol, H. T. Nembach, D. Rudolf, R. Adam, M. Aeschlimann, C. M. Schneider, T. J. Silva, M. M. Murnane, H. C. Kapteyn, and S. Mathias, *Phys. Rev. Lett.* **110**, 197201 (2013).
- [18] B. Koopmans, H. H. J. E. Kicken, M. van Kampen, and W. J. M. de Jonge, *J. Magn. Magn. Mater.* **286**, 271 (2005).
- [19] D. Steiauf and M. Fähnle, *Phys. Rev. B* **79**, 140401 (2009).
- [20] D. Steiauf, C. Illg, and M. Fähnle, *J. Magn. Magn. Mater.* **322**, L5 (2010).
- [21] M. Fähnle and C. Illg, *J. Phys. Condens. Matter* **23**, 493201 (2011).
- [22] B. Y. Mueller, A. Baral, S. Vollmar, M. Cinchetti, M. Aeschlimann, H. C. Schneider, and B. Rethfeld, *Phys. Rev. Lett.* **111**, 167204 (2013).
- [23] M. Battiato, K. Carva, and P. M. Oppeneer, *Phys. Rev. Lett.* **105**, 027203 (2010).
- [24] A. Melnikov, I. Razzdolski, T. O. Wehling, E. Th. Papaioannou, V. Roddatis, P. Fumagalli, O. Aktsipetrov, A. I. Lichtenstein, and U. Bovensiepen, *Phys. Rev. Lett.* **107**, 076601 (2011).
- [25] M. Battiato, K. Carva, and P. M. Oppeneer, *Phys. Rev. B* **86**, 024404 (2012).
- [26] A. J. Schellekens, W. Verhoeven, T. N. Vader, and B. Koopmans, *Appl. Phys. Lett.* **102**, 252408 (2013).
- [27] The local magnetic moments of  $3d$  TMs are known to remain stable even well above the Curie temperature  $T_C$ . In a previous density-functional study we have shown that the Ni moments are extremely stable even at very high levels of thermalized electronic excitation. See Ref. [28].
- [28] W. Töws and G. M. Pastor, *Phys. Rev. B* **86**, 054443 (2012).
- [29] A. J. Schellekens and B. Koopmans, *Phys. Rev. Lett.* **110**, 217204 (2013).
- [30] C. Illg, M. Haag, and M. Fähnle, *Phys. Rev. B* **88**, 214404 (2013).
- [31] T. Uchida and Y. Kakehashi, *Phys. Rev. B* **64**, 054402 (2001).
- [32] R. Garibay-Alonso, J. Dorantes-Dávila, and G. M. Pastor, *Phys. Rev. B* **91**, 184408 (2015).
- [33] Only in the presence of a very high point-group symmetry some component of  $\vec{L}$  may be conserved, for example,  $L_z$  in a linear chain along the  $z$  axis.
- [34] R. H. Victora and L. M. Falicov, *Phys. Rev. Lett.* **55**, 1140 (1985).
- [35] E. Dagotto, *Rev. Mod. Phys.* **66**, 763 (1994).
- [36] G. M. Pastor, R. Hirsch, and B. Mühlischlegel, *Phys. Rev. Lett.* **72**, 3879 (1994).
- [37] D. A. Papaconstantopoulos, *Handbook of the Band Structure of Elemental Solids* (Plenum Press, New York, 1986).
- [38] From atomic calculations one derives  $\xi \approx 70, 90$ , and  $110$  meV for Fe, Co, and Ni, respectively. See Ref. [39].
- [39] P. Bruno, *Magnetismus von Festkörpern und Grenzflächen* (KFA, Jülich, 1993), Chap. 24.
- [40] The sign of  $\xi$  can be changed by performing the electron-hole transformation  $\hat{h}_{i\alpha\sigma} = c_{i\alpha\sigma}^\dagger$ , which does not affect the Coulomb interaction and only changes the sign of the hopping integrals. Thus, band fillings above one-half can be simulated with less than one fermion per orbital. We have

explicitly checked that changing the sign of  $\xi$  does not affect the time dependence of the discussed observables in any significant way, except for the change of the relative orientation between  $\vec{s}_i$  and  $\vec{l}_i$ .

- [41] D. J. Tannor, *Introduction to Quantum Mechanics: A Time-Dependent Perspective* (University Science Books, Sausalito, California, 2007).
- [42] It has been explicitly checked that reasonable changes in the model parameters do not affect our physical conclusions.
- [43] G. P. Zhang and Thomas F. George, *Phys. Rev. B* **78**, 052407 (2008). This work shows that breaking the full rotational symmetry is necessary in order to allow for changes in the magnetization during the absorption of linearly polarized light.
- [44] L. D. Landau and E. M. Lifshitz, *Quantum Mechanics, Non-Relativistic Theory* (Pergamon, Oxford, 1958).
- [45] See Supplemental Material at <http://link.aps.org/supplemental/10.1103/PhysRevLett.115.217204> for the angular-momentum dynamics in the limit  $t_{ij}^{\alpha\beta} \rightarrow 0$ .